Design of a multiplex ligation-dependent probe amplification assay for SLC20A2: identification of two novel deletions in primary familial brain calcification

Design of a Multiplex Ligation-dependent Probe Amplification assay for *SLC20A2*: identification of two novel deletions in Primary Familial Brain Calcification.

Elisa Giorgio[1], Emanuela Garelli[2], Adriana Carando[2], Stefania Bellora[3], Elisa Rubino[4], Paola Quarello[2], Fabio Sirchia[5], Federico Marrama[6], Salvatore Gallone[7], Enrico Grosso[8], Barbara Pasini[1,8], Roberto Massa[6], Alessandro Brussino[1], Alfredo Brusco[1,8]

[1] Department of Medical Sciences, University of Torino, Turin, Italy.

[2] Department of Public Health and Pediatric Sciences, University of Torino, Turin, Italy.

[3] Pediatric Neuropsychiatry Unit, "SS Antonio e Biagio e Cesare Arrigo" Hospital, Alessandria, Italy.

[4]Department of Neuroscience and Mental Health, AOU Città della Salute e della Scienza di Torino

[5] Institute for Maternal and Child Health IRCCS Burlo Garofalo, Trieste, Italy

[6] Department of Systems Medicine, University of Rome Tor Vergata, Rome, Italy.

[7] Department of Neuroscience "Rita Levi Montalcini", University of Torino, Turin, Italy.

[8] Medical Genetics Unit, Città della Salute e della Scienza University Hospital, Turin, Italy.

Total word Count: 2628

Running title: MLPA for *SLC20A2*

Key words: SLC20A2, Primary Familial Brain Calcification, Fahr's syndrome, basal ganglia calcification, migraines, bipolar disorder

Corresponding author: Alfredo Brusco, University of Torino, Department of Medical Sciences, via Santena 19, 10126, Torino, Italy. Fax: 00390112365926. E-mail: alfredo.brusco@unito.it

ABSTRACT

Primary Familial Brain Calcification (PFBC) is a rare disease characterized by brain calcifications that mainly affect the basal ganglia, thalamus, and cerebellum. Among the four autosomal-dominant genes known to be associated with the disease, *SLC20A2* pathogenic variants are the most common, accounting for up to 40% of PFBC dominant cases; variants include both point mutations, small insertions/deletions and intragenic deletions. Over the last 7 years, we have collected a group of 50 clinically-diagnosed PFBC patients, who were screened for single nucleotide changes and small insertions/deletions in *SLC20A2* by Sanger sequencing. We found seven pathogenic/likely pathogenic variants: four were previously described by our group, and three are reported here (c.303delG, c.21delG, and c.1795-1G>A). We developed and validated a synthetic Multiplex Ligation-dependent Probe Amplification (MLPA) assay for *SLC20A2* deletions, covering all ten coding exons and the 5' UTR (*SLC20A2*-MLPA). Using this method, we screened the 43 PFBC-patients negative for point mutations and small insertions/deletions, and identified two novel intragenic deletions encompassing exon 6 NC_000008.10:g.(42297172_42302163)_(423022281_42317413)del, and exons 7-11 including the 3'UTR NC_000008.10:g.(?_42275320)_(42297172_42302163)del. Overall, *SLC20A2* deletions may be highly underestimated PFBC cases, and we suggest MLPA should be included in the routine molecular test for PFBC diagnosis.

INTRODUCTION

Primary Familial Brain Calcification (PFBC) is a rare clinically and genetically heterogeneous disorder characterized by primary symmetric and bilateral brain calcifications predominantly affecting the basal ganglia, thalamus, and cerebellum(1). The age of onset ranges from early childhood to ~80 yrs and is typically between 30 and 50 yrs with a median of 31 yrs (2). Clinical manifestations at onset are variable, the most frequent being psychiatric signs (70-80% of cases), movement disorders (40-77% of cases), and cognitive impairment (40-65% of cases) (2).

Diagnosing PFBC is supported by Computed Tomography (CT) detection of cerebral calcifications, and confirmed by identifying a causative mutation in one of the four known autosomal dominant PFBC-related genes, which account for up to 50% of familial cases (1, 3), namely the Solute Carrier Family 20, member 2 gene (*SLC20A2*) in IBGC type 1 or IBCG1 (MIM #213600), the platelet-derived growth factor receptor beta gene (*PDGFRB*) in IBGC4 (MIM #615007), the platelet-derived growth factor, beta polypeptide gene (*PDGFB*) in IBGC5 (MIM #615483) and the xenotropic and polytropic retrovirus receptor gene (*XPR1*) in IBGC6 (MIM #616413). A fifth subtype, IBCG2 (MIM #606656), has been mapped on chromosome 2q37 but no causative gene has been identified to date. A recessive form of PFBC (IBGC7; MIM#618317) has been recently associated to homozygous or compound heterozygous variants in the *MYORG* gene (4-7). Among the dominant genes known to be affected in patients with PFBC, mutations are most commonly found in *SLC20A2*, accounting for up to 40% of familial cases (3, 8, 9). A total of 62 different *SLC20A2* point mutations and small insertions/deletions have been reported so far (HGMD Professional 2018.2). Mutagenesis analysis of PiT-2 (10), *Slc20a2* knockout mice experiments (11), and partial SLC20A2 deletions in patients with PFBC (8) indicate that the underlying pathogenic mechanism is haploinsufficiency in SLC20A2-related PFBC. The worldwide distribution of *SLC20A2* variants does not suggest the presence of founder effects (12). In

the last two years, seven different intragenic *SLC20A2* deletions in PFBC patients have been reported (8, 13-15), suggesting that a strategy for detecting copy number variations (CNVs) should be included in the genetic diagnostics workup of PFBC.

Here, we developed and validated a synthetic Multiplex Ligation-dependent Probe Amplification (MLPA) assay designed to easily and cost-effectively identify intragenic *SLC20A2* deletions in routine clinical practice. Our results further support the importance of determining *SLC20A2* deletions in the diagnostic process of PFBC.

MATERIALS AND METHODS

Patients and Sanger sequencing

A total of 50 independent patients with clinically suspected PFBC due to the presence of brain calcifications at CT scan with or without clinical manifestations (1) were referred to our Genetic Unit between 2012 and 2018 (Table S3). All participants and/or their legal guardian/s provided written informed consent for the molecular analyses; the study was approved by the Internal Review Board of the Department of Medical Sciences, University of Torino, Italy. Experiments were performed in accordance with the relevant guidelines and regulations.

DNA samples were extracted from the blood using the Maxwell 16 system (Promega, Madison, WI, USA). Amplification and Sanger sequencing of all coding exons and flanking intron boundaries of *SLC20A2* (NM_006749; NP_006740.1) were performed as previously described (16). Sequences were analyzed using the SeqScape, v2.6 Software (Thermo Fisher Scientific, Foster City, CA, USA).

Multiplex Ligation-dependent Probe Amplification (MLPA)

MLPA oligonucleotide probes were designed according to the "Designing synthetic MLPA probes" protocol v.15 (MRC-Holland, Amsterdam, The Netherlands). Synthetic probes were created that were 98-150 nucleotides in size. Primers were synthesized by Integrated DNA Technologies (IDT, Leuven, Belgium) as PAGE Ultramer ® DNA Oligo, 4 nmole Ultramer ® DNA Oligo or 25 nmole DNA Oligo. Each synthetic probe was formed by two oligonucleotides, namely Left Probe Oligonucleotide (LPO) and Right Probe Oligonucleotide (RPO). LPOs were designed with a universal 5′-GGGTTCCCTAAGGGTTGGA sequence and a target-specific sequence. RPOs were designed with the target specific sequence followed by the universal 5'-TCTAGATTGGATCTTGCTGGCAC sequence (Table S1). We designed probes to detect all coding exons of the gene and the 5'-UTR region, which contains the active *SLC20A2* promoter and the putative regulatory elements (13), and corresponds to exon 1 of both the canonical (NM_006749) and the non-canonical (NM_001257180) transcript (probe SLC-1.1 and SLC-1.2, Table S1). Three reference probes, unrelated to PFBC, with a unique sequence specific for the Ribosomal Protein S19 (*RPS19*) and the Ribosomal Protein S26 (*RPS26*) genes, were added to the *SLC20A2*-specific panel as internal controls (Ref1, 2 and 3; Table S1). MLPA was performed using 50 ng of genomic DNA according to the manufacturer's instructions. The P200-A1 Human DNA reference kit (MRC-Holland), which includes reference probes, control fragments to verify DNA concentration and denaturation as well as Y-specific and X-specific control probes, was included in each reaction for correct copy number quantification.

PCR products were diluted at 1:7 in water; a volume of 1 µL was added to 10 µL of HiDi formamide (Thermo Fisher Scientific), and 0.1 µL of 500 ROX size standard (Thermo Fisher Scientific). Capillary electrophoresis was performed using the ABI PRISM 3130XL Genetic Analyzer, the POP7 polymer, and the MLPA run method (Thermo Fisher Scientific). Subsequent analyses were performed using GeneMapper 4.0 Software (Thermo Fisher Scientific). Following Coffalyzer (www.coffalyzer.net)

calculations, we performed for each sample: (i) an intra-normalization dividing the peak height of each probe amplification product by the total peak heights of all reference probes (Ref 1, 2, 3, and P200 Ref probes); (ii) an inter-sample normalization dividing the intra-normalized value of each probe by the average intra-normalized probe ratio of all control samples (at least three different healthy subjects for each experiment were considered). A no-DNA sample was run in each experiment as a negative control.

Threshold values were ≤0.7 for a loss (deletion) and ≥1.3 for gain (duplication) of genetic material. All samples showing evidence of a Copy Number Variant (CNV) were replicated on a second DNA extraction and validated by Real-Time quantitative PCR (see below).

Real-Time quantitative PCR validation of MLPA results

Validation of CNVs was performed by quantitative RT-PCR using the Universal Probe Library system (UPL, Roche, Mannheim, Germany) (Table S1) (17, 18). Reactions were carried out in triplicate on an ABI 7500 real-time PCR machine (Thermo Fisher Scientific), and at least two normal controls (calibrators) were added to each reaction. The gene dosage calculation strategy was based on the relative amplification of the target sequence (i.e., specific *SLC20A2* exons) and the co-amplified internal standard (*RNaseP*, Thermo Fisher Scientific) using the delta-delta Ct method (19, 20).

RESULTS

Identification of point mutations and small insertions/deletions in the SLC20A2 gene by Sanger sequencing

Over the last 7 years, we have collected a group of 50 clinically-diagnosed PFBC patients, who were screened for single nucleotide changes or small insertions/deletions of *SLC20A2* by Sanger sequencing.

We found seven pathogenic/likely pathogenic variants, four of which were previously described by our group (16, 21). Three additional variants are reported here, namely two frameshifts [c.303delG (p.W101Cfs*3); c.21delG (p.L7Ffs*10)], and one variant affecting the acceptor splice site of exon 11 (c.1795-1G>A) (submitted to ClinVar)(Table 1).

All seven *SLC20A2* patients exhibited severe calcifications involving the globus pallidus, caudate nuclei, putamen, thalamus and/or dentate nuclei, revealed by CT scan or MRI examination, in agreement with the clinical diagnosis of PFBC (16, 21) (Figure S1).

Patient PFBC-43-TO, carrying the c.303delG (p.W101Cfs*3) variant, is a 16-year-old girl of Italian origin presenting with a 2-year history of migraine, characterized by pulsating pain of moderate-to-severe intensity in the bilateral frontotemporal region, associated with severe nausea and photo/phonophobia. CT scan showed symmetrical bilateral calcifications at the frontal subcortical region and at the internal capsule, with a stronger density in the left hemisphere. Laboratory tests were normal. The c.303delG change is not present in public databases of healthy individuals (GnomAD, http://gnomad.broadinstitute.org/) (22). This single nucleotide deletion was predicted to alter the amino acid at position 101 and to insert a stop codon after two residues, likely leading to degradation of the mutated RNA messenger due to nonsense-mediated decay. Based on the rules outlined by the American College of Medical Genetics and Genomics (ACMG), the variant was classified as a class 5 mutation (pathogenic) (23).

Patient PFBC-49-TO, carrying the c.1795-1G>A splicing variant, is a 61-year-old asymptomatic woman. A CT scan performed after a head trauma showed a pattern of basal ganglia calcifications indicative of PFBC. The c.1795-1G>A variant is not present in public databases of healthy individuals (GnomAD, http://gnomad.broadinstitute.org/) (22), and is predicted to cause the loss of the acceptor

splice site, probably generating a messenger RNA lacking exon 11 and the 3'UTR of the *SLC20A2* gene. Based on ACMG rules, this variant was classified as a class 5 variant (pathogenic) (23).

Patient PFBC-50-TO, carrying the c.21delG (p.L7Ffs*10) frameshift variant, is a 61-year-old Italian woman from the Calabria region presenting with a 10-year history of involuntary movements of the left lower limb exclusively occurring when going down the stairs (24). This particular form of dystonia (called "down the stairs" dystonia) was characterized by extension of the left leg at the knee, along with plantar flexion and eversion of the foot at the ipsilateral ankle. Neurological examination was normal except for deep tendon hyperreflexia. Serum parathyroid hormone, alkaline phosphatase, calcium, phosphate and magnesium levels were all within normal ranges, but vitamin D was mildly reduced. A brain CT scan showed bilateral hyperdensities that were symmetrically located in the caudate nucleus, globus pallidus, thalamus and dentate nucleus. The proband had a negative family history for neurological or psychiatric diseases. The c.21delG change is not present in public databases of healthy individuals (GnomAD, http://gnomad.broadinstitute.org/) (22), but was previously reported to segregate in a southern Italian family presenting with familial PFBC (25). Based on ACMG rules, the variant was classified as a class 5 mutation (pathogenic) (23).

Setting up of an MLPA assay for the SLC20A2 gene

The probe mix of *SLC20A2*-specific custom probes and the P200 reference kit was tested on two control samples to assess its reliability and consistency (Figure 1). Standard deviations (SD) of the ratio for each of the 26 probes were calculated testing ten healthy individuals. Each probe showed a maximum coefficient of variation of 11.5%; normalized peak heights ranged from 0.74 to 1.16 (Table

S2, reference value for a deletion < 0.7; reference value for a duplication > 1.3). Data analyses were performed using an in-house developed Microsoft Excel sheet (available upon request).

Identification of SLC20A2 intragenic CNVs by MLPA

We performed *SLC20A2*-MLPA analysis on the 43 PFBC cases negative for single nucleotide variants and small insertion/deletions that can be detected by Sanger sequencing. Two samples were positive for intragenic deletions in the *SLC20A2* gene. Patient PFBC-01-TO carried a deletion from exon 7 to the 3'UTR region [NC_000008.10:g.(?_42275320)_(42297172_42302163)del] (Figure 1 and 2, Table 1; submitted to ClinVar); in patient PFBC-39-TO, we detected a deletion that encompassed only exon 6 [NC_000008.10:g.(42297172_42302163)_(423022281_42317413)del] (Figure 1 and 2, Table 1; submitted to ClinVar). Both deletions were validated by quantitative RT-PCR using *SLC20A2* exon-specific assays (Table S1). For patient PFBC-01-TO, we also verified if the deletion encompassed the 3'UTR by using a specific RT-PCR assay (Table S1). The breakpoints were not characterized at nucleotide level.

Patient PFBC-01-TO is a 48-year-old male Italian patient who was referred to the psychiatric ward due to an acute episode of psychosis at age 42 yrs. A CT scan performed at 42 yrs showed broad and diffuse calcifications in the cerebellum, basal ganglia, and subcortical regions. Neuropsychological examination revealed selective short-term memory deficits, while selective attention, learning skills and other cognitive functions were intact. Neurological examination was normal. Serum parathyroid hormone, alkaline phosphatase, calcium, phosphate and magnesium levels were all within normal ranges. A CT scan performed at 44 yrs showed multiple calcifications in the cerebellum and basal ganglia, suggesting a clinical diagnosis of PFBC. Neurological examination performed at 48 yrs showed severe cognitive decline with hyperactivity and anxiety, severe dysarthria and ataxia,

occasional dysphagia, and plastic hypertonia. The proband confirmed a positive family history for neurological disease: his father died at 50 yrs after a 6-year history of progressive cognitive decline. Genetic testing was not available at that time (1983). The *SLC20A2* deletion encompassed exons 7-11 and the 3'UTR of the gene [NC_000008.10:g.(?_42275320)_(42297172_42302163)del], as showed by real-time PCR analysis (data not shown). This rearrangement is predicted to generate a messenger RNA lacking the last five coding exons of the gene, likely leading to degradation of the mutated mRNA due to nonsense-mediated decay. Based on ACMG rules, the variant was classified as a class 5 variant (pathogenic) (23).

Patient PFBC-39-TO is a 66-year-old man of Italian origin with a long clinical history of migraine. At the last neurological examination, the proband presented with parkinsonism, and reported memory loss. The CT scan showed diffuse bilateral basal ganglia calcifications (globus pallidus, caudate nuclei, putamen, and bilateral thalamus). The proband had a positive family history for neurologic disease: his sister had a 6-year history of severe migraine. Her CT scan showed symmetrical basal ganglia calcifications, also affecting the thalamus and the cerebellar hemispheres in the posterior fossa. In both patients, a clinical diagnosis of PFBC was suggested.

The patient and his sister carried a deletion that exclusively encompassed exon 6 of the *SLC20A2* gene [NC_000008.10:g.(42297172_42302163)_(423022281_42317413)del], causing a predicted in-frame deletion of 39 amino acids (p.V205_G244delinsG). Based on other pathogenic variants already described in PFBC patients causing in-frame deletions and resulting in a loss of PiT-2 function (c.124_126delGTG) (10), (c.1470_1478delGCAGGTCCT) (26), (deletion of exons 4-5) (8) , on the recently described family with PFBC and a deletion encompassing exon 6 of the *SLC20A2* gene (15), and on the segregation of the mutation in the affected sister, we considered this deletion as pathogenic.

DISCUSSION

SLC20A2 represents the major causative gene in PFBC, accounting for the underlying cause in up to 40% of patients. More than 60 different point mutations and small insertions/deletions have been identified in this gene, resulting in impaired phosphate transport and its accumulation in the extracellular matrix of affected brain regions (10, 11). Seven different *SLC20A2* intragenic deletions have been reported, so far (8, 13-15) (Figure 2B); six of these encompass one or more coding exons, causing a frameshift with a premature stop codon, an in-frame large deletion, or eliminating the start codon located in exon 2 (8, 14, 15). The seventh is a noncoding CNV that abolishes the 5'UTR of the *SLC20A2* gene (exon 1) and extends upstream; this deletion probably disrupts the regulatory control regions of the gene (13). Moreover, two large genomic deletion encompassing multiple genes (seven and twenty-one, respectively) including *SLC20A2* have been described (15, 27). These CNVs and loss-of-function point mutations and small insertions/deletions support haploinsufficiency of *SLC20A2* as the pathogenic mechanism in PFBC.

Strategies to detect CNVs are therefore necessary to complement sequencing in genetic screening of PFBC. Consequently, we have developed an MLPA assay for the *SLC20A2* gene. Our probemix tests the non-coding 5' regulatory elements and the ten coding exons, allowing detection of both partial and whole-gene *SLC20A2* deletions. Compared to other strategies to quantify gene-dosage, such as real-time PCR, MLPA is cost-effective, reliable, and rapid allowing the relative quantification of different DNA target sequences in a single reaction. The *SLC20A2*-MLPA kit was initially validated on DNA samples from healthy subjects, and subsequently exploited in our routine genetic screening for PFBC patients.

Our patients with clinically suspected PFBC were analyzed for *SLC20A2* point mutations and small insertions/deletions, and negative cases were screened using *SLC20A2*-MLPA. This combined

approach allowed us to find *SLC20A2* causative variants in 18% (9/50) of unrelated probands from our cohort, in agreement with a recent paper reporting *SLC20A2*-mutations in 30 out of 177 (16.9%) unrelated probands with a clinical diagnosis of PFBC regardless of their family history (28). Among these nine, seven patients carried a pathogenic/likely pathogenic variant (7/50, 14%), and two had an intragenic deletion (2/50, 4%). These two deletion carriers would have been misdiagnosed as false negatives before the introduction of MLPA in our molecular diagnostic routine process. The detection rate of *SLC20A2* pathogenic variants increased to 46% (6/13) when only familial cases were considered. Notably, no data on family history were available for the three remaining *SLC20A2*-mutated patients.

Clinically, our mutation-positive cases confirmed the clinical heterogeneity of *SLC20A2*-associated PFBC. No phenotypic differences were present in case bearing deletions, compared with those carrying point mutations (2).

In conclusion, we have designed the first MLPA kit for identifying copy number variants in the *SLC20A2* gene. Together with published data, our work suggests that *SLC20A2* deletions may be overlooked because sequencing-based genetic analysis cannot detect disease-causing CNVs. Thus, we recommend *SLC20A2*-MLPA as a second-tier molecular test for PFBC diagnosis.

DISCLOSURE OF CONFLICTS OF INTEREST: None.

ACKNOWLEDGEMENTS

We are grateful to the participating families. This work was supported by Fondazione Umberto Veronesi (Postdoctoral Fellowship 2017) to E. Giorgio; Ricerca Locale MURST ex 60% and the "Associazione E.E. Rulfo per la ricerca biomedica" to A. Brusco; Ministero dell'Istruzione,

dell'Università e della Ricerca – MIUR "Dipartimenti di eccellenza 2018-2020" to Department of Medical Sciences- University of Torino (Project D15D18000410001).

DATA AVAILABILITY STATEMENT

The authors confirm that the data supporting the findings of this study are available within the article and its supplementary material.

REFERENCES

1. Westenberger A, Balck A, Klein C. Primary familial brain calcifications: genetic and clinical update. Current opinion in neurology. 2019;32(4):571-8.
2. Nicolas G, Charbonnier C, de Lemos RR, Richard AC, Guillin O, Wallon D, et al. Brain calcification process and phenotypes according to age and sex: Lessons from SLC20A2, PDGFB, and PDGFRB mutation carriers. Am J Med Genet B Neuropsychiatr Genet. 2015;168(7):586-94.
3. Legati A, Giovannini D, Nicolas G, Lopez-Sanchez U, Quintans B, Oliveira JR, et al. Mutations in XPR1 cause primary familial brain calcification associated with altered phosphate export. Nat Genet. 2015;47(6):579-81.
4. Arkadir D, Lossos A, Rahat D, Abu Snineh M, Schueler-Furman O, Nitschke S, et al. MYORG is associated with recessive primary familial brain calcification. Annals of clinical and translational neurology. 2019;6(1):106-13.
5. Forouhideh Y, Muller K, Ruf W, Assi M, Seker T, Tunca C, et al. A biallelic mutation links MYORG to autosomal-recessive primary familial brain calcification. Brain : a journal of neurology. 2019;142(2):e4.
6. Peng Y, Wang P, Chen Z, Jiang H. A novel mutation in MYORG causes primary familial brain calcification with central neuropathic pain. Clinical genetics. 2019;95(3):433-5.
7. Yao XP, Cheng X, Wang C, Zhao M, Guo XX, Su HZ, et al. Biallelic Mutations in MYORG Cause Autosomal Recessive Primary Familial Brain Calcification. Neuron. 2018;98(6):1116-23 e5.
8. David S, Ferreira J, Quenez O, Rovelet-Lecrux A, Richard AC, Verin M, et al. Identification of partial SLC20A2 deletions in primary brain calcification using whole-exome sequencing. Eur J Hum Genet. 2016;24(11):1630-4.
9. Hsu SC, Sears RL, Lemos RR, Quintans B, Huang A, Spiteri E, et al. Mutations in SLC20A2 are a major cause of familial idiopathic basal ganglia calcification. Neurogenetics. 2013;14(1):11-22.
10. Wang C, Li Y, Shi L, Ren J, Patti M, Wang T, et al. Mutations in SLC20A2 link familial idiopathic basal ganglia calcification with phosphate homeostasis. Nat Genet. 2012;44(3):254-6.
11. Jensen N, Schroder HD, Hejbol EK, Fuchtbauer EM, de Oliveira JR, Pedersen L. Loss of function of Slc20a2 associated with familial idiopathic Basal Ganglia calcification in humans causes brain calcifications in mice. J Mol Neurosci. 2013;51(3):994-9.
12. Lemos RR, Ramos EM, Legati A, Nicolas G, Jenkinson EM, Livingston JH, et al. Update and Mutational Analysis of SLC20A2: A Major Cause of Primary Familial Brain Calcification. Hum Mutat. 2015;36(5):489-95.

13. Pasanen P, Makinen J, Myllykangas L, Guerreiro R, Bras J, Valori M, et al. Primary familial brain calcification linked to deletion of 5' noncoding region of SLC20A2. Acta neurologica Scandinavica. 2017;136(1):59-63.
14. Grutz K, Volpato CB, Domingo A, Alvarez-Fischer D, Gebert U, Schifferle G, et al. Primary familial brain calcification in the 'IBGC2' kindred: All linkage roads lead to SLC20A2. Movement disorders : official journal of the Movement Disorder Society. 2016;31(12):1901-4.
15. Guo XX, Su HZ, Zou XH, Lai LL, Lu YQ, Wang C, et al. Identification of SLC20A2 deletions in patients with primary familial brain calcification. Clinical genetics. 2019.
16. Rubino E, Giorgio E, Gallone S, Pinessi L, Orsi L, Gentile S, et al. Novel mutation of SLC20A2 in an Italian patient presenting with migraine. J Neurol. 2014;261(10):2019-21.
17. Di Gregorio E, Riberi E, Belligni EF, Biamino E, Spielmann M, Ala U, et al. Copy number variants analysis in a cohort of isolated and syndromic developmental delay/intellectual disability reveals novel genomic disorders, position effects and candidate disease genes. Clinical genetics. 2017;92(4):415-22.
18. Di Gregorio E, Savin E, Biamino E, Belligni EF, Naretto VG, D'Alessandro G, et al. Large cryptic genomic rearrangements with apparently normal karyotypes detected by array-CGH. Mol Cytogenet. 2014;7(1):82.
19. Biamino E, Di Gregorio E, Belligni EF, Keller R, Riberi E, Gandione M, et al. A novel 3q29 deletion associated with autism, intellectual disability, psychiatric disorders, and obesity. Am J Med Genet B Neuropsychiatr Genet. 2016;171(2):290-9.
20. Bartoletti-Stella A, Gasparini L, Giacomini C, Corrado P, Terlizzi R, Giorgio E, et al. Messenger RNA processing is altered in autosomal dominant leukodystrophy. Hum Mol Genet. 2015;24(10):2746-56.
21. Rubino E, Giorgio E, Godani M, Grosso E, Zibetti M, Lopiano L, et al. Three novel missense mutations in SLC20A2 associated with idiopathic basal ganglia calcification. Journal of the neurological sciences. 2017;377:62-4.
22. Lek M, Karczewski KJ, Minikel EV, Samocha KE, Banks E, Fennell T, et al. Analysis of protein-coding genetic variation in 60,706 humans. Nature. 2016;536(7616):285-91.
23. Richards S, Aziz N, Bale S, Bick D, Das S, Gastier-Foster J, et al. Standards and guidelines for the interpretation of sequence variants: a joint consensus recommendation of the American College of Medical Genetics and Genomics and the Association for Molecular Pathology. Genet Med. 2015;17(5):405-24.
24. Menon S, Muglan JA, Shimon L, Stewart D, Snow B, Hayes M, et al. Down the Stairs Dystonia - A Novel Task-Specific Focal Isolated Syndrome. Movement disorders - Clinical Practice. 2016;4(1):121-4.
25. Gagliardi M, Morelli M, Annesi G, Nicoletti G, Perrotta P, Pustorino G, et al. A new SLC20A2 mutation identified in southern Italy family with primary familial brain calcification. Gene. 2015;568(1):109-11.

26. Chen WJ, Yao XP, Zhang QJ, Ni W, He J, Li HF, et al. Novel SLC20A2 mutations identified in southern Chinese patients with idiopathic basal ganglia calcification. Gene. 2013;529(1):159-62.
27. Baker M, Strongosky AJ, Sanchez-Contreras MY, Yang S, Ferguson W, Calne DB, et al. SLC20A2 and THAP1 deletion in familial basal ganglia calcification with dystonia. Neurogenetics. 2014;15(1):23-30.
28. Ramos EM, Carecchio M, Lemos R, Ferreira J, Legati A, Sears RL, et al. Primary brain calcification: an international study reporting novel variants and associated phenotypes. Eur J Hum Genet. 2018;26(10):1462-77.

FIGURE LEGENDS

Figure 1. *SLC20A2*-MLPA profiles. Panels show the analysis of two controls, two PFBC patients carrying an intragenic *SLC20A2* deletion, and a no-DNA sample, using the GeneMapper 4.0 Software. Q-fragments, custom probes (*SLC20A2*-specific and the internal reference- Ref1, Ref2 and Ref3-probes), and P200 reference fragments are shown. Y-specific and X-specific control probes and custom internal reference peaks are highlighted (black arrows). Peaks corresponding to deleted exons in patients PFBC-01-TO and PFBC-39-TO are indicated with red arrows. Sizes and IDs of MLPA peaks are reported on the Table on the right.

Figure 2. MLPA results and summary of known *SLC20A2* intragenic deletions.

Panel A. Histogram plots showing the results of MLPA analysis of two controls (Female CTR and Male CTR) and the two patients carrying a *SLC20A2* intragenic deletion (PFBC-01-TO and PFBC-39-TO). The x-axis shows the probe names; the y-axis shows the fold-change (gene dosage). Intra- and inter-normalizations have been performed as described in the "Materials and Methods" section. Threshold values of loss and gain of a genetic material were set at 0.7 (shown as a horizontal black line) and 1.30 (not shown in the figure), respectively. The exons deleted in patients PFBC-01-TO and PFBC-39-TO are indicated with red bars. *SLC20A2*-specific probes are in blue, covering the 5' UTR (exons 1.1 and 1.2) and all ten coding exons. Dashed boxes represent our custom probe mix (*SLC20A2*-specific probes and the three reference probes, in purple). In green, the commercially available P200 DNA reference probes.

Panel B. In-scale schematic representation of *SLC20A2* mRNA (NM_006749). The horizontal blue bar represents the whole messenger RNA. The 5' and 3' untranslated regions are reported as dashed boxes.

Coding exons are in light blue. The exon number (1-11) is reported inside each box. The number of the first and last cDNA nucleotide is shown for each coding exon. The first Methionine (ATG, blue arrowhead) and the translational stop codon (TGA, blue square) are displayed. At the bottom, all published *SLC20A2* intragenic deletions are reported as orange bars, together with the literature reference. Red bars represent the two deletions identified in this paper.

Figure 1.

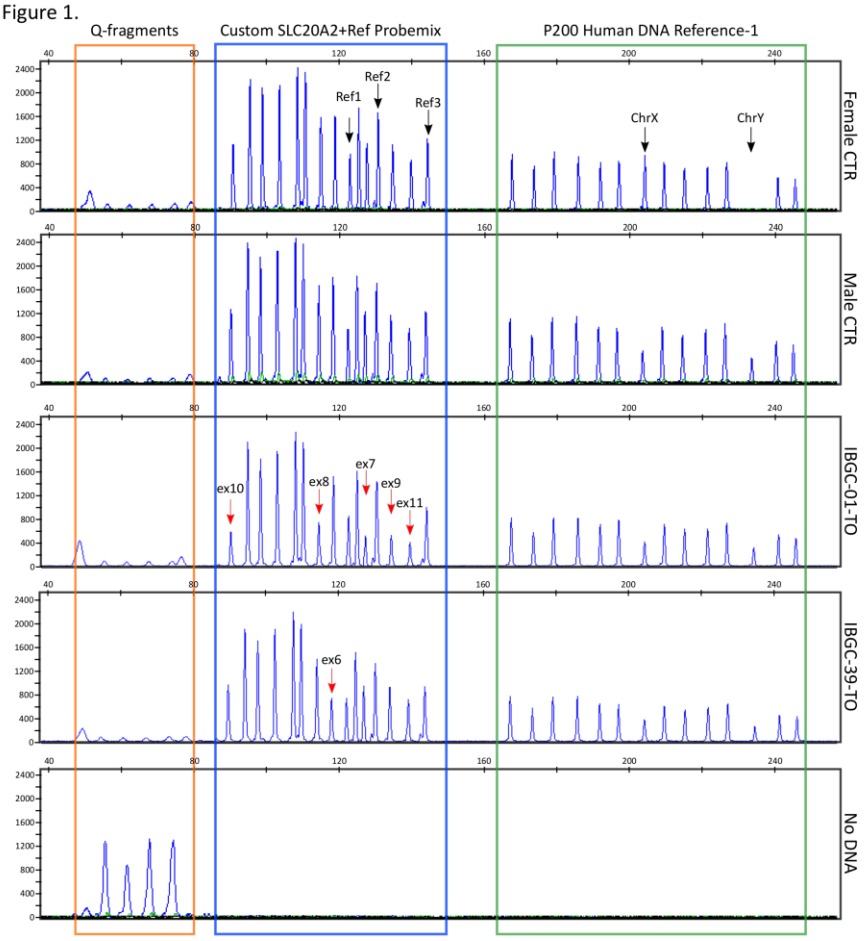

Peak	
Size	ID
66.47	Q-fragment
72.86	Q-fragment
79.27	Q-fragment
85.00	Q-fragment
95.25	SLC-10
99.88	SLC-2
103.38	SLC-1.1
108.02	SLC-3
113.14	SLC-4
115.20	SLC-5
119.44	SLC-8
123.47	SLC-6
127.00	Ref1
129.97	SLC-1.2
132.19	SLC-7
135.00	Ref2
139.26	SLC-9
144.39	SLC-11
149.00	Ref3
172.18	REF 7q
178.24	REF 14q
183.80	D-fragment
190.53	REF 20p
196.53	REF 13q
201.62	REF 20p
208.76	chrX
214.07	REF10p
219.59	REF 12q
225.98	REF 4q
231.29	REF 18q
238.67	chrY
245.39	REF 5p
250.06	REF 17p

Table 1. Patients reported in the manuscript with a pathogenic variant.

ID	Sex	Symptom at onset	Variant	Positive family history	Previous ID
IBGC-01-TO	M	psychosis	ex7-11del; c.(730+1_731-1)_(*1_?)del	yes	
IBGC-04-TO	F	headache	p.Val507Glufs*2	yes	Patient 1 in [6]
IBGC-06-TO	F	headache	p.Gly63Asp	yes	case 1 in [8]
IBGC-17-TO	M	bipolar disorder	p.Gly63Ser	yes	case 2 in [8]
IBGC-19-TO	F	migraines without aura	p.His399Pro	NA	case 3 in [8]
IBGC-39-TO	M	migraines	ex6del; c.(613+1_614-1)_(730+1_731-1	yes	
IBGC-43-TO	F	migraines	p.Trp101Cysfs*3	yes	
IBGC-49-TO	F	asymptomatic	c.1795-1 G>A	NA	
IBGC-50-TO	F	stairs dystonia	p.Leu7Phefs*10	no	

Table S1. MLPA probes and real-time PCR primers and UPL probes

oligo ID	gene	position	transcript ID	synthesis scale	Seq modification	sequence 5' - 3'
LPO-SLC-1.1	SLC20A2	Canonical exon 1	NM_006749	25 nmole DNA oligo	none	GGGTTCCCTAAGGGTTGC
LPO-SLC-1.2	SLC20A2	Alternative exon 1	NM_001257180	25 nmole DNA oligo	none	GGGTTCCCTAAGGGTTGC
LPO-SLC-2	SLC20A2	exon 2	NM_006749	25 nmole DNA oligo	none	GGGTTCCCTAAGGGTTGC
LPO-SLC-3	SLC20A2	exon 3	NM_006749	25 nmole DNA oligo	none	GGGTTCCCTAAGGGTTGC
LPO-SLC-4	SLC20A2	exon 4	NM_006749	25 nmole DNA oligo	none	GGGTTCCCTAAGGGTTGC
LPO-SLC-5	SLC20A2	exon 5	NM_006749	25 nmole DNA oligo	none	GGGTTCCCTAAGGGTTGC
LPO-SLC-6	SLC20A2	exon 6	NM_006749	4 nmole Ultramer DNA oligo	none	GGGTTCCCTAAGGGTTGC
LPO-SLC-7	SLC20A2	exon 7	NM_006749	4 nmole Ultramer DNA oligo	none	GGGTTCCCTAAGGGTTGC
LPO-SLC-8	SLC20A2	intron 8	NM_006749	25 nmole DNA oligo	none	GGGTTCCCTAAGGGTTGC
LPO-SLC-9	SLC20A2	exon 9	NM_006749	4 nmole Ultramer DNA oligo	none	GGGTTCCCTAAGGGTTGC
LPO-SLC-10	SLC20A2	exon 10	NM_006749	25 nmole DNA oligo	none	GGGTTCCCTAAGGGTTGC
LPO-SLC-11	SLC20A2	exon 11	NM_006749	4 nmole Ultramer DNA oligo	none	GGGTTCCCTAAGGGTTGC
LPO-Ref1	RPS26	exon 4	NM_001029	4 nmole Ultramer DNA oligo	none	GGGTTCCCTAAGGGTTGC
LPO-Ref2	RPS26	exon 1	NM_001029	4 nmole Ultramer DNA oligo	none	GGGTTCCCTAAGGGTTGC
LPO-Ref3	RPS19	exon 1	NM_001022	4 nmole Ultramer DNA oligo	none	GGGTTCCCTAAGGGTTGC
RPO- SLC-1.1	SLC20A2	Canonical exon 1	NM_006749	PAGE Ultramer DNA oligo	5'Phosphorylation	TGAACTCTTCCAGTCTTGG
RPO- SLC-1.2	SLC20A2	Alternative exon 1	NM_001257180	PAGE Ultramer DNA oligo	5'Phosphorylation	TGGTAGGATATCTATTTTA
RPO- SLC-2	SLC20A2	exon 2	NM_006749	PAGE Ultramer DNA oligo	5'Phosphorylation	TTTAGCTTCAATATTTGAA
RPO- SLC-3	SLC20A2	exon 3	NM_006749	PAGE Ultramer DNA oligo	5'Phosphorylation	CACTGCATTGTGGGTTCTA
RPO- SLC-4	SLC20A2	exon 4	NM_006749	PAGE Ultramer DNA oligo	5'Phosphorylation	TGGTTTCATGTCTGGCCTG
RPO- SLC-5	SLC20A2	exon 5	NM_006749	PAGE Ultramer DNA oligo	5'Phosphorylation	AGCAATCAATGTCTTTTCC
RPO- SLC-6	SLC20A2	exon 6	NM_006749	PAGE Ultramer DNA oligo	5'Phosphorylation	CCAAAACCTCACATGTAAC
RPO- SLC-7	SLC20A2	exon 7	NM_006749	PAGE Ultramer DNA oligo	5'Phosphorylation	GAAGCAGAGTCCCCAGTAT
RPO- SLC-8	SLC20A2	intron 8	NM_006749	PAGE Ultramer DNA oligo	5'Phosphorylation	GGGATAGGGGTGCGCAGG
RPO- SLC-9	SLC20A2	exon 9	NM_006749	PAGE Ultramer DNA oligo	5'Phosphorylation	CGAGGCCTGGGTAGAGCTT
RPO- SLC-10	SLC20A2	exon 10	NM_006749	PAGE Ultramer DNA oligo	5'Phosphorylation	CGATCGAGCTGGCCTCAGC
RPO- SLC-11	SLC20A2	exon 11	NM_006749	PAGE Ultramer DNA oligo	5'Phosphorylation	AGCGCTGCTGTCATGGCTC
RPO-Ref1	RPS26	exon 4	NM_001029	PAGE Ultramer DNA oligo	5'Phosphorylation	TACATCAGTTTGTGAGAGG
RPO-Ref2	RPS26	exon 1	NM_001029	PAGE Ultramer DNA oligo	5'Phosphorylation	CAGAAATGCTGAATGTAAA
RPO-Ref3	RPS19	exon 1	NM_001022	PAGE Ultramer DNA oligo	5'Phosphorylation	GTTCCCTGTCACAGTTCCG

UPL Real-time PCR probes and primers

oligo ID	position	transcript ID	UPL probe	sequence 5' - 3'
SLC-ex6F	upstream exon 6	NM_006749	48	TGACCTTGCAGAAGTTTCCAG
SLC-ex6R	exon 6	NM_006749	48	CCCACATGGGGAGAACAA
SLC-ex7F	downstream exon 7	NM_006749	57	AGGCTCACTCTTGTCCTGTGA
SLC-ex7R	downstream exon 7	NM_006749	57	TGGGTGCAGCACAGACATAC
SLC-ex11F	upstream exon 11	NM_006749	77	GTTTTTACTTTGCAATGTCTGCTC
SLC-ex11R	exon 11	NM_006749	77	CGAAGATGTTCCGAAAGAGG
SLC-3utrF	3'utr	NM_006749	42	GAGAGGGAGGGAGAATCCTG
SLC-3utrR	3'utr	NM_006749	42	GGGTGTCCAGCTTTGTGTG

Table S2. Size of the MLPA probes

		PEAK SIZE		PEAK HEIGHT	
	probe ID	**expected**	**observed**	**Mean±SD**	**Range**
SLC20A2 probes	SLC-10	98	95.25	0.880±0.079	0.797-0.993
	SLC-2	102	99.88	0.913±0.101	0.767-1.088
	SLC-1.1	106	103.38	0.898±0.098	0.743-1.05
	SLC-3	110	108.02	0.919±0.088	0.796-1.054
	SLC-4	114	113.14	0.941±0.081	0.812-1.056
	SLC-5	118	115.2	0.933±0.096	0.776-1.081
	SLC-8	122	119.44	0.907±0.104	0.787-1.07
	SLC-6	126	123.47	0.944±0.075	0.837-1.056
	Ref1	129	127	0.969±0.063	0.866-1.083
	SLC-1.2	131	129.97	0.958±0.080	0.816-1.068
	SLC-7	135	132.19	0.975±0.065	0.889-1.087
	Ref2	138	135	0.971±0.091	0.859-1.095
	SLC-9	140	139.26	0.965±0.076	0.878-1.066
	SLC-11	144	144.39	0.971±0.067	0.886-1.066
	Ref3	150	149	1.008±0.074	0.938-1.117
P200 probes	REF 7q	173	172.18	1.021±0.029	0.963-1.071
	REF 14q	178	178.24	0.958±0.034	0.905-1.014
	D-fragment	184	183.8		
	REF 20p	190	190.53	1.020±0.046	0.961-1.1
	REF 13q	196	196.53	1.001±0.047	0.939-1.067
	REF 20p	202	201.62	1.011±0.050	0.926-1.081
	chr X	208	208.76		
	REF 10p	214	214.07	0.966±0.048	0.899-1.032
	REF 12q	220	219.59	1.013±0.041	0.95-1.099
	REF 4q	226	225.98	1.021±0.065	0.919-1.101
	REF 18q	233	231.29	1.034±0.059	0.928-1.1
	chrY	240	238.67		
	REF 5p	244	245.39	1.032±0.112	0.869-1.157
	REF 17p	250	250.06	1.012±0.109	0.843-1.156

Note: Total probe length represents the total length of amplification product = forward primers + upstream hybridizing sequence + downstream hybridizing sequence + reverse primers